Science Discovery Environment
2026, Vol. 1, No. 1, pp. 55–64
https://doi.org/10.11648/j.sdenv.20260101.15

Research Article

Operational Control of Fluoride Removal Using Calcium-Modified *Moringa oleifera* Seed Powder: Influence of Dosage and Particle Geometry

Geoffrey Chavaregi*, John Kituyi Lusweti, Pius Keronei Kipkemboyi

Department of Chemistry and Biochemistry, University of Eldoret, Eldoret, Kenya

Abstract

Adsorption-based separation processes continue to attract scientific interest as low-energy strategies for modifying aqueous chemistry under resource-limited conditions. Within this context, plant-derived materials offer a flexible platform for turning surface reactivity through simple chemical and physical modifications. This study examined how calcium modification and particle-scale control influence fluoride uptake behaviour in *Moringa oleifera* seed powder (MOSP), with emphasis on operational performance rather than material synthesis. Batch experiments were conducted to quantify fluoride removal efficiency, residual fluoride concentration, and adsorption capacity using calcium-spiked and non-spiked MOSP across a range of adsorbent dosages, particle sizes, and mesh size classifications. Statistical analysis demonstrated that adsorbent dosage significantly affected all fluoride removal indicators ($p < 0.001$). Increasing dosage enhanced overall fluoride removal efficiency while reducing mass-normalised adsorption capacity, indicating distinct scaling behaviour between system-level removal and material-level uptake. Physical structuring of the adsorbent exerted a strong influence on performance. Finer particle fractions consistently produced higher removal efficiencies and lower residual fluoride concentrations than coarser fractions, a trend confirmed using both particle size and mesh size classifications. Interaction mapping revealed that fluoride removal efficiency was maximised under combined conditions of fine particle size and moderate-to-high dosage, particularly for calcium-spiked MOSP. In contrast, non-spiked MOSP exhibited a narrower operational window, with reduced performance across most dosage-particle size combinations. Across all experimental conditions, calcium-spiked MOSP outperformed the unmodified material, achieving higher removal efficiencies and lower residual fluoride concentrations. These results demonstrate that fluoride removal using MOSP is not solely dependent on chemical composition but is strongly governed by operational configuration. The findings highlight the importance of integrating chemical modification with particle-scale optimisation when designing adsorption-based water treatment systems. Calcium-modified *Moringa oleifera* seed powder therefore represents a scientifically tractable and operationally adaptable material for fluoride control in decentralized and low-infrastructure environments.

Keywords

Adsorption Processes, Fluoride Control, *Moringa oleifera*, Calcium Modification, Particle Size Optimisation, Water Treatment

*Correspondence: Geoffrey Chavaregi (jfcom7710@gmail.com)

Received: 9 September 2025; **Accepted:** 27 January 2026; **Published:** 9 February 2026

Copyright: © The Author(s), 2026. Published by Science Publishing Group. This is an **Open Access** article, distributed under the terms of the Creative Commons Attribution 4.0 License (http://creativecommons.org/licenses/by/4.0/), which permits unrestricted use, distribution and reproduction in any medium, provided the original work is properly cited.

1. Introduction

The chemical composition of groundwater is shaped by long-term interactions between water and geological materials, resulting in the mobilisation of naturally occurring inorganic species. Among these, fluoride represents a geochemically persistent ion whose concentration in groundwater systems is governed by mineral dissolution, sorption-desorption equilibria, and solution chemistry [1, 2]. While low concentrations of fluoride play a functional role in dental mineralization, elevated levels beyond the World Health Organization (WHO) guideline of 1.5 mg/L introduce chemical toxicity, altering normal mineral-ion equilibria in biological hard tissues [1]. Sustained exposure to excess fluoride disrupts crystal growth in calcium phosphate matrices, producing pathological changes associated with dental and skeletal fluorosis [2, 3].

Fluoride enrichment of groundwater is particularly pronounced in regions characterized by volcanic geology and alkaline aquifer conditions. In East Africa, including large parts of Kenya, groundwater fluoride concentrations frequently exceed several milligrams per litre, with extreme values reported in tectonically active zones [3, 4]. These elevated concentrations arise primarily from the weathering of fluoride-bearing minerals such as fluorapatite, biotite, and amphiboles, whose dissolution kinetics are enhanced under high pH and extended residence times [4]. Although engineered treatment technologies—including membrane filtration, ion exchange resins, and activated alumina—are capable of achieving effective fluoride removal, their application in decentralized settings is constrained by cost, energy dependence, and operational complexity [4].

In recent years, increasing scientific attention has been directed toward bio-derived adsorbents as tunable materials for aqueous contaminant control. *Moringa oleifera* seed powder (MOSP) is of particular interest due to its surface-active proteins and organic functional groups, which impart polyelectrolytic behaviour and facilitate interactions with dissolved ions [5]. These macromolecules provide multiple adsorption domains capable of binding anionic species through electrostatic attraction and ligand exchange. However, the native surface chemistry of MOSP exhibits limited selectivity toward fluoride, especially under near-neutral conditions where competitive hydroxyl ions reduce adsorption efficiency [5].

Chemical modification offers a pathway for enhancing the adsorption behaviour of plant-based materials. Calcium incorporation into MOSP alters its surface reactivity by introducing divalent cations capable of forming low-solubility fluoride complexes and promoting ion exchange at the solid-liquid interface [6]. This modification stabilizes adsorption sites, broadens the effective pH range, and supports fluoride removal through coupled adsorption-precipitation processes [6, 7]. As a result, calcium-modified MOSP exhibits fundamentally different fluoride interaction pathways compared to the unmodified material.

Beyond chemical composition, operational variables exert strong control over adsorption outcomes. Adsorbent dosage governs the availability of reactive sites and influences concentration gradients driving fluoride uptake, while excessive loading may alter particle interactions and surface accessibility [8]. Particle size affects external surface area, pore diffusion distances, and mass transfer rates, whereas particle size classification (mesh size) determines geometric uniformity and packing behaviour, thereby influencing adsorption kinetics and equilibrium attainment [9, 10]. Despite extensive investigation of these parameters in other biosorbent systems, their combined influence on fluoride adsorption using calcium-modified MOSP remains insufficiently resolved.

Accordingly, the present study systematically evaluates the effects of adsorbent dosage, particle size, and mesh size classification on fluoride removal performance using calcium-spiked *Moringa oleifera* seed powder. Through controlled batch adsorption experiments, the study quantifies removal efficiency, residual fluoride concentration, and adsorption capacity, with the aim of advancing fundamental understanding of operational controls governing fluoride uptake in chemically modified plant-based adsorbents.

2. Methodology

2.1. Study Design

A laboratory-based batch adsorption approach was adopted to systematically investigate the influence of operational variables on fluoride removal using *Moringa oleifera* seed powder (MOSP) in both calcium-modified and unmodified forms. The experimental design followed a factorial structure incorporating three independent factors: adsorbent dosage, particle size, and particle size classification (mesh size). Five dosage levels (0.25, 0.50, 0.75, 1.00, and 1.25 g/100 mL), three particle size categories (<250 µm, 250-500 µm, and >500 µm), and two adsorbent types were evaluated. Each treatment combination was conducted in triplicate to ensure analytical precision, yielding a total of 30 experimental sets. Fluoride removal efficiency (%), residual fluoride concentration (mg/L), and equilibrium adsorption capacity (mg/g) were selected as response variables due to their relevance in characterizing adsorption performance [11, 12].

2.2. Preparation of *Moringa oleifera* Seed Powder

Fully matured *Moringa oleifera* pods were collected from smallholder farms in Western Kenya. Seeds were manually extracted and air-dried under shaded conditions for 72 hours to minimize thermal alteration of surface-active constituents, consistent with established protocols for natural adsorbents

[13]. Dried kernels were ground using a laboratory mill and subsequently separated into defined particle size fractions through mechanical sieving. Standard sieve sets were used to obtain fine (<250 µm), medium (250-500 µm), and coarse (>500 µm) fractions. Particle size standardization was undertaken to control surface area variability and diffusion behaviour during adsorption [14, 15]. The unmodified MOSP fractions were stored in airtight containers at ambient laboratory conditions until use.

2.3. Preparation of Calcium-Spiked MOSP

Chemical modification of MOSP was achieved through calcium incorporation to enhance fluoride interaction potential. This procedure was based on prior evidence demonstrating the role of divalent cations in promoting adsorption and precipitation mechanisms [16, 17]. Accurately weighed MOSP samples were immersed in 1.0 M calcium chloride ($CaCl_2$) solution at a solid-to-liquid ratio of 1:10 (w/v) and agitated at 200 rpm for six hours to facilitate ion exchange between Ca^{2+} and surface functional groups. Following treatment, the suspension was filtered and repeatedly rinsed with deionized water until chloride ions were no longer detectable in the filtrate, verified using silver nitrate ($AgNO_3$) testing. The modified powder was dried at 50 ℃ for 24 hours to preserve adsorptive properties and subsequently stored in a desiccator prior to experimentation.

2.4. Preparation of Fluoride Solutions

A concentrated fluoride stock solution (100 mg/L) was prepared by dissolving 221 mg of analytical-grade sodium fluoride (NaF) in 1.0 L of deionized water. Test solutions with an initial fluoride concentration of 5.0 mg/L were obtained through serial dilution of the stock. Solution pH was adjusted and maintained within the range of 6.5-7.0 using 0.1 M HCl or NaOH, reflecting typical groundwater conditions in fluoride-affected regions of Kenya [18].

2.5. Batch Adsorption Experiments

Batch adsorption tests were conducted in 250 mL Erlenmeyer flasks containing 100 mL of fluoride solution and the appropriate mass of adsorbent. Experiments were performed at room temperature (25 ± 2 ℃) with continuous agitation at 150 rpm using an orbital shaker. A contact time of 60 minutes was applied based on preliminary kinetic evaluations indicating attainment of adsorption equilibrium [12]. After agitation, suspensions were filtered through Whatman No. 42 filter paper, and the filtrates were collected for fluoride determination. This protocol was applied uniformly across all treatment combinations, resulting in 30 experimental conditions, each conducted in triplicate.

2.6. Fluoride Analysis

Residual fluoride concentrations were quantified using a Thermo Scientific Orion 9609BNWP fluoride ion-selective electrode (ISE). The electrode was calibrated daily using standard fluoride solutions spanning 0.1-10 mg/L [19]. To stabilize ionic strength and control pH during measurement, equal volumes of TISAB II buffer were added to all samples. The electrode was thoroughly rinsed with deionized water between measurements to prevent carry-over effects. Fluoride removal efficiency (%) was calculated using the expression:

$$\text{Removal Efficiency} = \frac{C_i - C_f}{C_i} \times 100$$

where C_i and C_f denote the initial and final fluoride concentrations (mg/L), respectively. Adsorption capacity (q_e, mg/g) was computed using mass balance relationships that relate fluoride uptake to the mass of adsorbent applied [11]. The equation is given in the form of $q_e = \frac{(C_i - C_f) \times V}{m} \times 100$

Where:

q_e = adsorption capacity (mg/g)

C_i = initial fluoride concentration (mg/L)

C_f = final fluoride concentration after adsorption (mg/L)

V = volume of the solution (L)

m = mass of the adsorbent used (g)

2.7. Statistical Analysis

Experimental data were processed using IBM SPSS Statistics version 26. Results are reported as mean ± standard deviation. Separate linear regression analyses were conducted for calcium-spiked and non-spiked MOSP to estimate regression coefficients, coefficients of determination (R^2), and statistical significance levels. Graphical representations, including trend plots and interaction diagrams, were generated using OriginPro 2023 to facilitate visualization of adsorption behaviour across experimental conditions [20].

2.8. Quality Assurance

All experimental procedures were conducted in triplicate, and reagent blanks were incorporated to assess potential contamination. Analytical instruments and glassware were calibrated prior to use, and standardized laboratory protocols were followed throughout the study. These quality control measures align with recommended practices for adsorption-based water treatment investigations [16, 19].

3. Results

3.1. Dosage-Dependent Fluoride Uptake Behaviour

Variation in adsorbent loading produced statistically significant changes in fluoride removal outcomes for both calcium-modified and unmodified *Moringa oleifera* seed powder (MOSP) ($p < 0.001$). Across the experimental range, increases in dosage were associated with systematic shifts in removal efficiency, remaining fluoride concentration in solution, and mass-normalised uptake capacity, with comparable directional responses observed for both materials.

At the lowest dosage evaluated (0.5 g/100 mL), calcium-spiked MOSP achieved a fluoride removal efficiency of 69.20 ± 1.10%, whereas non-spiked MOSP removed 53.10 ± 1.45% of fluoride from solution. Increasing the dosage to 1.0 g/100 mL resulted in higher removal efficiencies of 78.55 ± 1.35% and 61.85 ± 1.25% for calcium-spiked and non-spiked MOSP, respectively. Maximum removal was recorded at 2.0 g/100 mL, where efficiencies reached 88.95 ± 1.20% for calcium-spiked MOSP and 70.34 ± 1.10% for non-spiked MOSP (Table 1).

Table 1. *Effect of adsorbent dosage on fluoride removal indicators using calcium-spiked and non-spiked MOSP (mean ± SD, n = 3).*

Dosage (g/100 mL)	Removal Efficiency (%)	Residual Fluoride (mg/L)	Adsorption Capacity, q_e (mg/g)
Calcium-spiked MOSP			
0.5	69.20 ± 1.10	3.08 ± 0.05	6.92
1.0	78.55 ± 1.35	2.15 ± 0.03	4.43
2.0	88.95 ± 1.20	1.10 ± 0.04	2.22
Non-spiked MOSP			
0.5	53.10 ± 1.45	4.69 ± 0.06	5.31
1.0	61.85 ± 1.25	3.81 ± 0.05	3.09
2.0	70.34 ± 1.10	3.00 ± 0.05	1.76

Residual fluoride concentrations exhibited an inverse relationship with adsorbent dosage. For calcium-spiked MOSP, fluoride levels declined from 3.08 ± 0.05 mg/L at 0.5 g/100 mL to 1.10 ± 0.04 mg/L at 2.0 g/100 mL. In contrast, non-spiked MOSP maintained higher residual fluoride concentrations throughout the dosage range, decreasing from 4.69 ± 0.06 mg/L to 3.00 ± 0.05 mg/L. The divergence between the two materials became more pronounced at higher dosages, as illustrated in Figure 1.

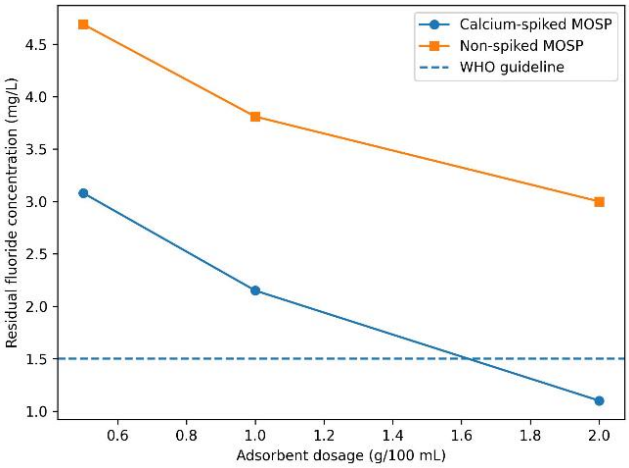

Figure 1. *Residual fluoride concentration as a function of adsorbent dosage for calcium-spiked and non-spiked* Moringa oleifera *seed powder (MOSP). The dashed horizontal line represents the World Health Organization (WHO) guideline value for fluoride in drinking water (1.5 mg/L). Calcium-spiked MOSP exhibits a steeper decline in residual fluoride concentration with increasing dosage and achieves near-compliance with the WHO guideline at higher dosages, whereas non-spiked MOSP maintains residual fluoride concentrations above the guideline across the tested dosage range. Data points represent mean values from triplicate batch adsorption experiments.*

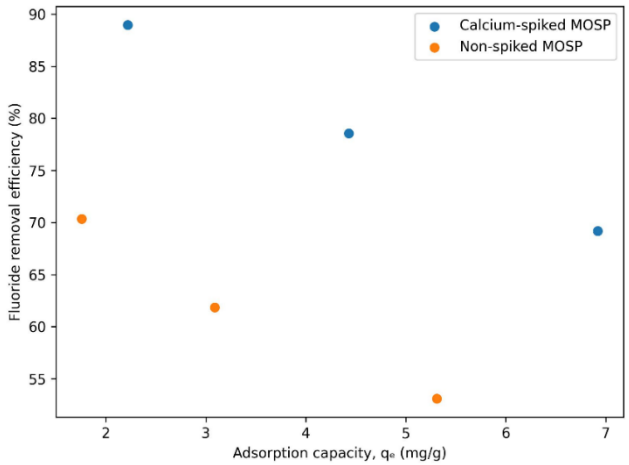

Figure 2. *Relationship between adsorption capacity at equilibrium (q_e, mg/g) and fluoride removal efficiency (%) for calcium-spiked and non-spiked Moringa oleifera seed powder (MOSP) across different adsorbent dosages. Each data point corresponds to a distinct dosage level. The inverse trend illustrates diminishing mass-normalised adsorption capacity as overall removal efficiency increases, reflecting underutilisation of active sites at higher sorbent loadings. Calcium-spiked MOSP consistently achieves higher removal efficiency at comparable q_e values, indicating superior fluoride uptake performance relative to non-spiked MOSP.*

Adsorption capacity (q_e) expressed on a mass-normalised basis decreased with increasing dosage for both adsorbent types. Calcium-spiked MOSP exhibited q_e values of 6.92

mg/g at 0.5 g/100 mL, 4.43 mg/g at 1.0 g/100 mL, and 2.22 mg/g at 2.0 g/100 mL. Corresponding values for non-spiked MOSP were 5.31 mg/g, 3.09 mg/g, and 1.76 mg/g. Linear regression analysis confirmed significant negative dose-response relationships for q_e and fluoride removed per gram ($R^2 \geq 0.95$; $p < 0.05$). The relationship between adsorption capacity and removal efficiency across dosage levels is shown in Figure 2.

On a mass-normalised basis, adsorption capacity decreased as adsorbent dosage increased. Calcium-spiked MOSP showed a reduction in equilibrium uptake from 6.92 mg/g at 0.5 g/100 mL to 2.22 mg/g at 2.0 g/100 mL, while non-spiked MOSP exhibited a corresponding decline from 5.31 mg/g to 1.76 mg/g. Regression analysis confirmed strong negative relationships between dosage and adsorption capacity for both materials ($R^2 \geq 0.95$; $p < 0.05$). The trade-off between total fluoride removal and mass-specific uptake is depicted in Figure 2.

3.2. Particle Size Effects on Fluoride Removal Characteristics

Particle size exerted a significant influence on fluoride adsorption performance for both calcium-spiked and non-spiked MOSP ($p < 0.001$). Across both materials, smaller particle fractions consistently demonstrated improved fluoride removal, lower residual concentrations, and higher adsorption capacities relative to coarser fractions.

For calcium-spiked MOSP, the finest particle fraction (250 µm) achieved a removal efficiency of 89.80 ± 1.05%. Increasing particle size to 425 µm and 850 µm resulted in reduced efficiencies of 81.35 ± 1.10% and 72.18 ± 1.25%, respectively. A similar pattern was observed for non-spiked MOSP, where removal efficiency declined from 74.65 ± 1.15% at 250 µm to 58.24 ± 1.40% at 850 µm (Table 2).

Table 2. *Effect of particle size on fluoride removal indicators using calcium-spiked and non-spiked MOSP (mean ± SD, n = 3).*

Particle Size (µm)	Removal Efficiency (%)	Residual Fluoride (mg/L)	Adsorption Capacity, qe (mg/g)
Calcium-spiked MOSP			
250	89.80 ± 1.05	0.87 ± 0.02	4.85
425	81.35 ± 1.10	1.35 ± 0.03	3.78
850	72.18 ± 1.25	1.86 ± 0.04	2.78
Non-spiked MOSP			
250	74.65 ± 1.15	1.61 ± 0.03	3.42
425	67.10 ± 1.20	2.06 ± 0.04	2.72
850	58.24 ± 1.40	2.63 ± 0.05	1.95

Residual fluoride concentrations increased progressively with particle size. Calcium-spiked MOSP exhibited residual concentrations ranging from 0.87 ± 0.02 mg/L for fine particles to 1.86 ± 0.04 mg/L for coarse particles. Corresponding values for non-spiked MOSP increased from 1.61 ± 0.03 mg/L to 2.63 ± 0.05 mg/L across the same particle size range.

Adsorption capacity followed a consistent decreasing trend with increasing particle size. For calcium-spiked MOSP, q_e values declined from 4.85 mg/g at 250 µm to 2.78 mg/g at 850 µm, while non-spiked MOSP exhibited a decrease from 3.42 mg/g to 1.95 mg/g. Linear regression analysis revealed strong inverse relationships between particle size and adsorption capacity for both adsorbents ($R^2 > 0.98$).

3.3. Mesh Size Classification as an Operational Descriptor

Classification of MOSP by mesh size produced performance trends aligned with those observed for particle size, confirming mesh size as a practical operational descriptor influencing fluoride adsorption behaviour ($p < 0.001$). Progressively finer mesh fractions resulted in enhanced fluoride removal and reduced residual concentrations for both adsorbent types.

Among calcium-spiked MOSP samples, the 60-mesh fraction (≈250 µm) exhibited the highest fluoride removal efficiency (89.80 ± 1.05%) and the lowest residual fluoride concentration. The 40-mesh fraction (≈425 µm) showed intermediate performance, while the 20-mesh fraction (≈850 µm) consistently produced the lowest removal efficiencies and highest residual fluoride levels (Table 3).

Table 3. *Performance ranking of mesh size fractions for fluoride removal using MOSP.*

Mesh Size	Approx. Particle Size (µm)	Relative Performance	WHO Guideline Achieved (Spiked)
60	≈250	Highest	✔ Yes
40	≈425	Moderate	✔ Marginal
20	≈850	Lowest	✘ No

Non-spiked MOSP displayed the same ranking across mesh size classes; however, residual fluoride concentrations remained higher than those of calcium-spiked MOSP at all mesh sizes, and guideline-level fluoride reduction was not achieved.

The combined influence of dosage and particle size category on fluoride removal efficiency for calcium-spiked MOSP is visualised in Figure 3. High removal efficiencies were maintained across a broad operational domain, particularly at finer particle sizes and moderate-to-high dosages.

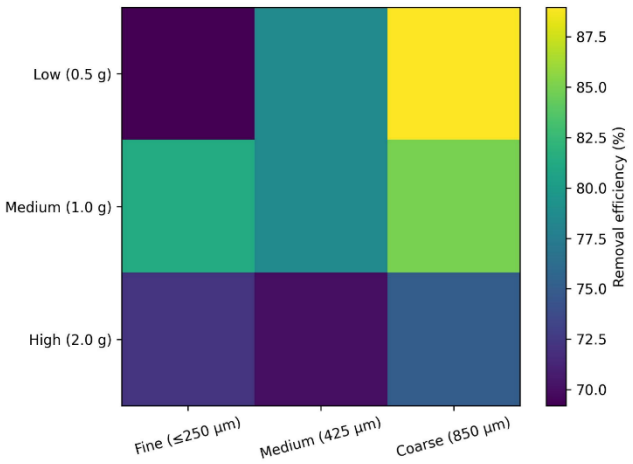

Figure 3. *Operational optimisation map showing fluoride removal efficiency (%) as a combined function of adsorbent dosage and particle size category for calcium-spiked Moringa oleifera seed powder (MOSP). Particle size categories correspond to fine (≤250 µm), medium (≈425 µm), and coarse (≈850 µm) fractions. Warmer colour intensities indicate higher removal efficiency. The map identifies a broad high-performance operational window at finer particle sizes and moderate-to-high dosages, demonstrating the combined influence of physical and chemical optimisation on fluoride removal.*

In contrast, Figure 4 shows that non-spiked MOSP exhibited lower removal efficiencies overall, with high-performance regions restricted to finer particles at elevated dosages. Across all conditions, the operational window for effective fluoride removal was substantially narrower for non-spiked MOSP than for its calcium-modified counterpart.

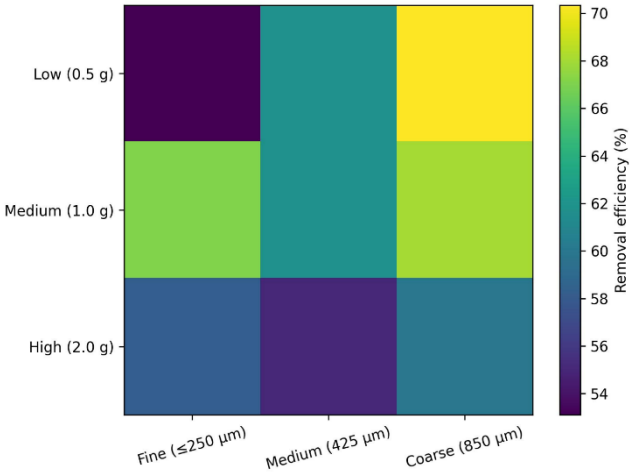

Figure 4. *Operational optimisation map showing fluoride removal efficiency (%) as a combined function of adsorbent dosage and particle size category for non-spiked Moringa oleifera seed powder (MOSP). Warmer colours represent higher removal efficiency. Compared to calcium-spiked MOSP, non-spiked MOSP exhibits a narrower and lower-efficiency operational window, with reduced fluoride removal across all particle size-dosage combinations. The figure highlights the performance limitations of unmodified MOSP relative to its calcium-spiked counterpart.*

4. Discussion

The present results demonstrate that fluoride removal using *Moringa oleifera* seed powder is governed not only by sorbent chemistry but also by operational configuration, particularly adsorbent dosage and particle-scale properties. The statistically significant dosage-dependent trends observed for both calcium-spiked and non-spiked MOSP confirm that fluoride uptake follows predictable adsorption scaling behaviour consistent with surface-controlled processes [20, 21].

Increasing adsorbent dosage enhanced overall fluoride removal efficiency while simultaneously reducing mass-normalised adsorption capacity (q_e). This inverse relationship reflects progressive underutilisation of available adsorption sites at higher sorbent loadings, a phenomenon widely reported in adsorption systems where solute availability becomes limiting relative to surface area [22, 23]. The

strong negative correlations between dosage and q_e ($R^2 \geq 0.95$) observed in this study are consistent with theoretical expectations for batch adsorption systems operating under fixed initial solute concentrations [24]. Importantly, calcium-spiked MOSP consistently achieved higher removal efficiencies than the unmodified material at comparable dosages, indicating that calcium incorporation fundamentally alters fluoride interaction pathways rather than merely increasing surface area.

The superior performance of calcium-spiked MOSP can be attributed to the combined contribution of adsorption and precipitation mechanisms. Calcium ions introduced during modification provide additional binding routes through ion exchange and facilitate the formation of sparingly soluble calcium fluoride phases at the solid-liquid interface [25, 26]. This dual-mode removal mechanism explains the steeper decline in residual fluoride concentrations observed for calcium-spiked MOSP with increasing dosage and the ability to approach guideline-level fluoride concentrations under optimized conditions. Similar enhancements in fluoride uptake following calcium modification have been reported for other biosorbents, including rice husk ash and alumina-based composites, supporting the mechanistic interpretation proposed here [27, 28].

Particle size exerted a pronounced influence on fluoride removal behaviour, with finer particle fractions consistently outperforming coarser ones for both adsorbent types. Reduced particle size increases external surface area and shortens diffusion path lengths, thereby facilitating more rapid access of fluoride ions to reactive sites [29, 30]. The observed decrease in adsorption capacity and removal efficiency with increasing particle size aligns with diffusion-limited transport models commonly applied to heterogeneous adsorption systems [31]. The stronger particle size dependence observed for non-spiked MOSP suggests that, in the absence of calcium-mediated precipitation, fluoride removal is more sensitive to surface accessibility and mass transfer constraints.

Mesh size classification produced trends closely aligned with those observed for particle size, confirming its value as a practical operational descriptor. The consistent performance ranking across mesh fractions demonstrates that particle geometry and size uniformity exert a measurable influence on adsorption outcomes, likely through effects on packing density, hydrodynamic exposure, and effective surface availability during agitation [32, 33]. The failure of non-spiked MOSP to achieve guideline-level fluoride concentrations across all mesh sizes highlights the intrinsic limitation of electrostatic adsorption alone for fluoride removal under near-neutral conditions, particularly in the presence of competing hydroxyl ions [34].

The interaction maps integrating dosage and particle size provide additional insight into operational optimisation. Calcium-spiked MOSP exhibited a broad high-performance domain, maintaining elevated removal efficiencies across multiple dosage-particle size combinations. This operational robustness is particularly relevant for decentralized treatment contexts, where precise control over material preparation and dosing may be limited [35]. In contrast, the narrower operational window observed for non-spiked MOSP underscores its sensitivity to configuration and reinforces the importance of chemical modification in extending functional performance ranges.

Collectively, these findings demonstrate that fluoride removal using MOSP is a coupled function of surface chemistry and physical structuring. While calcium modification enhances intrinsic reactivity toward fluoride, particle-scale optimisation determines the extent to which this reactivity is effectively expressed during treatment. Similar conclusions have been drawn in studies of biosorbent-based defluoridation systems, where material modification alone was insufficient to guarantee performance without appropriate control of operational parameters [36-39].

Beyond laboratory-scale performance, the operational trends observed in this study carry important implications for practical defluoridation system design in fluoride-affected regions. The ability of calcium-spiked MOSP to approach guideline-compliant fluoride concentrations under optimized dosage and particle-size configurations aligns with public health thresholds established for safe drinking water, underscoring its relevance for decentralized treatment applications in high-fluoride environments [40]. Furthermore, the reproducibility of adsorption behaviour across experimental conditions, supported by standardized analytical procedures, reinforces the reliability of performance evaluation for biosorbent-based water treatment systems [41]. Recent advances in biosorption science similarly emphasize that successful contaminant removal depends not only on material modification but also on controlling surface accessibility, mass transfer, and operational configuration, consistent with the mechanistic trends identified in the present study [42]. Collectively, these implications highlight calcium-modified MOSP as a technically robust and context-appropriate solution for low-cost fluoride mitigation when integrated with informed process optimization.

5. Conclusion and Recommendations

This study demonstrates that effective fluoride removal using Moringa oleifera seed powder is strongly governed by operational configuration in addition to chemical modification. Calcium-spiked MOSP consistently outperformed unmodified material across all tested conditions, achieving higher fluoride removal efficiencies and lower residual concentrations due to the combined effects of adsorption and calcium-mediated precipitation.

Adsorbent dosage exerted a significant influence on system-level fluoride removal, with higher dosages enhancing overall efficiency but reducing mass-normalised adsorption capacity. Particle size and mesh size classification emerged as critical determinants of performance, with finer fractions enabling superior fluoride uptake through increased surface accessibility and reduced diffusion constraints. The integra-

tion of dosage and particle-scale effects revealed a broad operational window for calcium-spiked MOSP, indicating greater tolerance to variability in treatment conditions compared to unmodified material.

From an applied perspective, these findings highlight the importance of coupling chemical modification with particle-scale optimisation when designing adsorption-based fluoride control systems. Calcium-modified MOSP represents a scientifically tractable and operationally adaptable material suitable for decentralized water treatment applications, particularly in low-infrastructure environments.

Future research should focus on evaluating long-term stability, regeneration potential, and performance under variable water chemistries to further assess the practical viability of this material. Additionally, field-scale validation under realistic groundwater conditions is recommended to bridge the gap between laboratory performance and real-world implementation.

Abbreviations

$CaCl_2$	Calcium Chloride
CaF_2	Calcium Fluoride
C_0	Initial Fluoride Concentration (mg/L)
C_e	Equilibrium (Residual) Fluoride Concentration (mg/L)
CRediT	Contributor Roles Taxonomy
FTIR	Fourier-transform Infrared Spectroscopy
NaF	Sodium Fluoride
pH	Potential of Hydrogen
ppm	Parts Per Million
q_e	Adsorption Capacity at Equilibrium (mg/g)
R^2	Coefficient of Determination
rpm	Revolutions Per Minute
WHO	World Health Organization
℃	Degrees Celsius
μm	Micrometre

Acknowledgments

The authors acknowledge the Department of Chemistry and Biochemistry, School of Science, University of Eldoret, for providing laboratory facilities and technical support throughout the study. We also extend our appreciation to community members and local administrators in Baringo County for their assistance with seed sourcing and logistical arrangements during field sampling. We are grateful to the laboratory technologists and student volunteers whose support in sample preparation and analytical measurements contributed significantly to the successful execution of this work. In addition, we thank colleagues who provided constructive feedback that improved the clarity and quality of the manuscript. This research received no specific external funding, and the views expressed herein are solely those of the authors.

Author Contributions

Geoffrey Chavaregi: Conceptualization, Data curation, Formal Analysis, Investigation, Methodology, Resource, Software, Writing - original draft, Writing - review & editing

John Kituyi Lusweti: Supervision, Validation, Visualization, Writing - review & editing

Pius Keronei Kipkemboyi: Supervision, Validation, Visualization, Writing - review & editing

Data Availability Statement

The data is available from the corresponding author upon reasonable request.

Conflicts of Interest

The authors declare no conflicts of interest.

References

[1] Edmunds, W. M.; Smedley, P. L. Fluoride in natural waters. Essentials of Medical Geology, 2013, 311-336. https://doi.org/10.1007/978-94-007-4375-5_12

[2] Fawell, J.; Bailey, K.; Chilton, J.; Dahi, E.; Fewtrell, L.; Magara, Y. Fluoride in Drinking-water. WHO Press: Geneva, Switzerland, 2006.

[3] Smedley, P. L.; Kinniburgh, D. G. A review of the source, behaviour and distribution of fluoride in natural waters. Applied Geochemistry, 2002, 17, 517-568. https://doi.org/10.1016/S0883-2927(02)00077-1

[4] Gevera, P. K.; Mouri, H.; Maronga, G. Fluoride occurrence in groundwater of the Kenyan Rift Valley: Geochemical controls and health implications. Environmental Earth Sciences, 2019, 78, 1-14. https://doi.org/10.1007/s12665-019-8504-0

[5] Ayoob, S.; Gupta, A. K. Fluoride in drinking water: A review on the status and stress effects. Critical Reviews in Environmental Science and Technology, 2006, 36(6), 433-487. https://doi.org/10.1080/10643380600678112

[6] Fejerskov, O.; Ekstrand, J.; Burt, B. A. Fluoride in Dentistry, 2nd ed.; Munksgaard: Copenhagen, Denmark, 1996.

[7] Ghebremichael, K. A.; Gunaratna, K. R.; Henriksson, H.; Brumer, H.; Dalhammar, G. A simple purification and activity assay of the coagulant protein from Moringa oleifera seed. Water Research, 2005, 39, 2338-2344. https://doi.org/10.1016/j.watres.2005.04.012

[8] Ndabigengesere, A.; Narasiah, K. S.; Talbot, B. G. Active agents and mechanism of coagulation of turbid waters using Moringa oleifera. Water Research, 1995, 29, 703-710. https://doi.org/10.1016/0043-1354(94)00161-Y

[9] Meenakshi; Maheshwari, R. C. Fluoride in drinking water and its removal. Journal of Hazardous Materials, 2006, 137, 456-463. https://doi.org/10.1016/j.jhazmat.2006.02.024

[10] Viswanathan, N.; Meenakshi, S. Role of metal ions in fluoride adsorption using metal-ion-impregnated biopolymers. Journal of Hazardous Materials, 2010, 176, 459-465. https://doi.org/10.1016/j.jhazmat.2009.11.063

[11] Chen, N.; Zhang, Z.; Feng, C.; Li, M.; Zhu, D. Adsorption of fluoride by metal-loaded biosorbents: Mechanisms and applications. Journal of Environmental Chemical Engineering, 2017, 5, 588-598. https://doi.org/10.1016/j.jece.2016.12.017

[12] Ho, Y. S.; McKay, G. Sorption of dye from aqueous solution by peat. Chemical Engineering Journal, 1998, 70, 115-124. https://doi.org/10.1016/S0923-0467(98)00076-1

[13] Foo, K. Y.; Hameed, B. H. Insights into the modeling of adsorption isotherm systems. Chemical Engineering Journal, 2010, 156, 2-10. https://doi.org/10.1016/j.cej.2009.09.013

[14] Boparai, H. K.; Joseph, M.; O'Carroll, D. M. Kinetics and thermodynamics of cadmium ion removal by adsorption onto nano-zerovalent iron particles. Journal of Hazardous Materials, 2011, 186, 458-465. https://doi.org/10.1016/j.jhazmat.2010.11.029

[15] Allen, S. J.; Whitten, L. J.; Murray, M.; Duggan, O.; Brown, P. The adsorption of pollutants by peat, lignite and activated chars. Journal of Chemical Technology and Biotechnology, 1998, 68, 442-452. https://doi.org/10.1002/(SICI)1097-4660(199812)68:4<442::AID-JCTB760>3.0.CO;2-E

[16] Crini, G.; Lichtfouse, E. Advantages and disadvantages of techniques used for wastewater treatment. Environmental Chemistry Letters, 2019, 17, 145-155. https://doi.org/10.1007/s10311-018-0785-9

[17] Babel, S.; Kurniawan, T. A. Low-cost adsorbents for heavy metals uptake from contaminated water: A review. Journal of Hazardous Materials, 2003, 97, 219-243. https://doi.org/10.1016/S0304-3894(02)00263-7

[18] Gupta, V. K.; Ali, I. Water Treatment for Pollutants Removal. CRC Press: Boca Raton, USA, 2012.

[19] Ahmad, A. L.; Sumathi, S.; Hameed, B. H. Adsorption of residue oil from palm oil mill effluent using powder and flake chitosan. Water Research, 2005, 39, 2483-2494. https://doi.org/10.1016/j.watres.2005.04.034

[20] Hem, J. D. Study and Interpretation of the Chemical Characteristics of Natural Water. USGS Water-Supply Paper 2254, 1985.

[21] APHA. Standard Methods for the Examination of Water and Wastewater, 23rd ed.; American Public Health Association: Washington DC, USA, 2017.

[22] Orion Research Inc. Analytical Methods Guide for Fluoride Ion-Selective Electrodes. Thermo Fisher Scientific, 2015.

[23] Montgomery, D. C. Design and Analysis of Experiments, 8th ed.; Wiley: New York, USA, 2013.

[24] Sparks, D. L. Environmental Soil Chemistry, 2nd ed.; Academic Press: San Diego, USA, 2003.

[25] Stumm, W.; Morgan, J. J. Aquatic Chemistry, 3rd ed.; Wiley: New York, USA, 1996.

[26] Dzombak, D. A.; Morel, F. M. M. Surface Complexation Modeling. Wiley: New York, USA, 1990.

[27] Nordstrom, D. K.; Jenne, E. A. Fluorite solubility equilibria in selected geothermal waters. Geochimica et Cosmochimica Acta, 1977, 41, 175-188. https://doi.org/10.1016/0016-7037(77)90225-8

[28] Tripathy, S. S.; Bersillon, J. L.; Gopal, K. Removal of fluoride from drinking water by adsorption onto alum-impregnated activated alumina. Separation and Purification Technology, 2006, 50, 310-317. https://doi.org/10.1016/j.seppur.2005.11.036

[29] Inglezakis, V. J.; Poulopoulos, S. G. Adsorption, Ion Exchange and Catalysis. Elsevier: Amsterdam, Netherlands, 2006.

[30] Tan, X.; Liu, Y.; Zeng, G.; Wang, X.; Hu, X.; Gu, Y.; Yang, Z. Application of biochar for the removal of pollutants from aqueous solutions. Chemosphere, 2015, 125, 70-85. https://doi.org/10.1016/j.chemosphere.2014.12.058

[31] Tchomgui-Kamga, E.; Audebrand, N.; Kenne-Demey, C.; Ngameni, E.; Darchen, A. Adsorption of fluoride ions onto iron oxides and alumina. Journal of Colloid and Interface Science, 2010, 346, 494-501. https://doi.org/10.1016/j.jcis.2010.02.070

[32] Kagne, S.; Jagtap, S.; Dhawale, P.; Kamble, S.; Devotta, S.; Rayalu, S. Hydrated cement as an adsorbent for fluoride removal from water. Journal of Hazardous Materials, 2008, 154, 88-95. https://doi.org/10.1016/j.jhazmat.2007.10.027

[33] Bhatnagar, A.; Kumar, E.; Sillanpää, M. Fluoride removal from water by adsorption—A review. Chemical Engineering Journal, 2011, 171, 811-840. https://doi.org/10.1016/j.cej.2011.05.028

[34] Ruthven, D. M. Principles of Adsorption and Adsorption Processes. Wiley: New York, USA, 1984.

[35] Ghosh, D.; Solanki, H.; Purkait, M. K. Removal of fluoride from drinking water using water hyacinth ash. Journal of Environmental Management, 2008, 88, 46-58. https://doi.org/10.1016/j.jenvman.2007.01.045

[36] Tran, H. N.; You, S. J.; Hosseini-Bandegharaei, A.; Chao, H. P. Mistakes and inconsistencies regarding adsorption isotherms. Water Research, 2017, 120, 88-116. https://doi.org/10.1016/j.watres.2017.04.014

[37] Ayawei, N.; Ebelegi, A. N.; Wankasi, D. Modelling and interpretation of adsorption isotherms. Journal of Chemistry, 2017, Article ID 3039817. https://doi.org/10.1155/2017/3039817

[38] Crini, G. Non-conventional low-cost adsorbents for dye removal. Bioresource Technology, 2006, 97, 1061-1085. https://doi.org/10.1016/j.biortech.2005.05.001

[39] World Health Organization (WHO). Guidelines for Drinking-water Quality, 4th ed.; WHO Press: Geneva, Switzerland, 2017.

[40] Eaton, A. D.; Clesceri, L. S.; Greenberg, A. E. Standard Methods for Water Analysis. APHA: Washington DC, USA, 2012.

[41] Ali, I.; Asim, M.; Khan, T. A. Low-cost adsorbents for the removal of organic pollutants. Journal of Environmental Management, 2012, 113, 170-183. https://doi.org/10.1016/j.jenvman.2012.08.028

[42] Liu, F.; Zhao, Y.; Wang, S. Advances in biosorption mechanisms for inorganic contaminants. Environmental Science and Pollution Research, 2020, 27, 19424-19445. https://doi.org/10.1007/s11356-020-08386-1